

## **6 Appendix – SCR Recording During fMRI Acquisition**

This work was conducted by Antoine Bruguier, R. McKell Carter, Christof Koch and Steven Quartz. Experiments were carried out at the Caltech Biological Imaging Center (CBIC) by AB, CK and RMC. Steve Flaherty and J. Michael Tyszka from the CBIC were also very helpful in conducting the experiments. Analysis and interpretation were conducted by all authors. The first draft of the text below was prepared by AB. Figures were prepared by AB and RMC. All authors were involved in the review of this manuscript. We also received assistance during the filter design process, specifically in how to ensure subject safety while using grounded filters, from Alan Macy of Biopac (Goleta, CA).

### **6.1 Abstract**

Investigative methods in neuroscience increasingly combine functional magnetic resonance imaging (fMRI) with other measurement and stimulus-delivery systems. Many of these, such as electroencephalography (EEG), electrocardiography (ECG) and skin conductance response (SCR) measurements, attach electrodes to subjects inside the strong variable magnetic field of the scanner. This may induce dangerous voltages on the leads that often go unassessed. While burn injuries and electric shocks have been reported, there is surprisingly little available research describing these risks. This paper presents a simple model of the human body and a filtering system that aims to assess these burn risks and prevent electrical shocks. The electrical properties of this setup and the induced voltages on the leads as measured in a variety of configurations, including the effect of fMRI transmitting and receiving coils and lead composition, are presented. Since these combined methods introduce noise that requires additional filtering, we also

studied the safety constraints of various filters. Even though the design methods and measurements are applied to a skin-conductance/shock delivery setup, they can be generalized to other systems for assessing and preventing risks associated with similar combined methods.

## **6.2 Introduction**

Many recording methods often combined with fMRI, such as EEG, GSR, and ECG, involve attaching leads to subjects. There are two main risks of having leads attached to subjects during MRI: inducing currents in leads that may cause sufficient heat to burn subjects, and creating an electrical current inside the subjects themselves. Despite these risks, we have not found any satisfactory studies of the risk inherent to attaching electrodes, since most references, such as (Shellock, 2000b, a), concentrate on safety regarding the specific absorption rate (SAR – the amount of radio frequency energy absorbed in tissue, usually watts per kilogram for a given volume) and implanted devices. The limitation on the SAR was implemented in order to reduce the heating of the subject's tissue, and is now regulated by the FDA. Ferromagnetic implants will experience an attractive force and may cause physical harm, and numerous cases of injuries and even deaths have been reported. For this reason, most research institutions screen subjects for implanted devices and virtually ban most of them. Burn injuries are not, however, limited to implanted devices, as the presence of electrodes is in itself a hazard. The FDA has reported excessive heating resulting in third degree burns in the case of an ECG connection (see for example report M765635 in their Medical Device Reporting database). Finally, the voltages created by the scanner create noise in the

recording devices. Given that the strong variable magnetic field inside a scanner may induce a voltage in any attached leads, such methods raise two important issues: 1) what are the direct safety consequences to the subject and 2) how can the noise such leads introduce be eliminated without causing further safety concerns?

As indicated above, the variable magnetic fields inside the scanner create substantial noise in the various recordings that should be filtered out to obtain a usable signal. A first step is to use analog filters before the actual recording takes place. Unfortunately, these filters have their own safety requirements. First, they usually require a ground connection, and one should be concerned about connecting a subject to a ground lead because there can be a voltage difference between a room ground and the ground conductor of a medical device. Subjects who are in contact with two unequal ground references may experience a leakage current. Second, these filters modify the recording circuit itself; therefore, the safety of the subject and the quality of the recordings should be jointly studied.

We here investigate these issues through two conjunctive methods: skin conductance recording, and the delivery of shocks in a scanner. Skin conductance recording is a fairly common conjunctive method that is used for peripheral correlates of emotional states, while shock delivery is increasingly used for behavioral conditioning and pain experiments (Carter et al., 2006). Although we focus on these two applications, these methods carry over to other applications.

## **6.3 Material and methods**

### **6.3.1 Equipment**

The full schematic of our equipment is shown in Figure 6-1. Two devices from Psylab (Psylab SAM, Boston MA), a skin conductance instrument and a shock delivery device, were powered through a PC-managed controller. In between the devices and the simulated subject we placed a low-pass filter that is described in more detail below. On the subject side of the filter, various types of leads were connected and attached to the simulated subject. A wave-guide served as the interface between the control room and the room where the scanner is located.

Since we use a 3T scanner (Siemens Trio), its Larmor frequency is ~123 MHz; thus, the values of components in the filters presented here are designed for such frequencies. Since there is variability in different institutions' hardware, only the methods can be generalized and the results should be investigated on a case-by-case basis.

### **6.3.2 Body simulation**

To simulate the electrical properties of a human body attached to pairs of leads, we used conductive electric paste. This paste, Med-Associates TD-246 (0.5M NaCl suspension), was originally designed to create contact between a subject and electrodes and has similar conductive properties to human perspiration. To mimic both hands, paste was placed in two plastic dishes on a strip approximately 4 inches long and 0.5 inch wide, resulting in a resistivity of approximately 30k $\Omega$ . These two dishes were then connected together by another strip of paste (0.25 inch wide and 16 inches long) to simulate a subject's chest (Figure 6-1). Since the magnetic fields increase with the proximity to the center of the

scanner, we placed this model in the approximate location a real subject's hands would be located in relation to the scanner center.

By using this “dummy”, we tried to mimic the various loops created by four leads. It should be noted that the model described above should be modified for other setups that include more leads.

### **6.3.3 Leads and electrodes**

Since the behavior of various lead materials within the scanner is not firmly established, we used a number of different leads (custom made by InVivo Metric, Healdsburg, CA, and Biopac Systems Inc, Santa Barbara, CA) to investigate the extent of induced voltages in them. We tested regular copper wires (30 foot, 16 AWG), short (6 foot) carbon fiber leads extended by 24 foot-long regular copper wires, and full-length (30 foot) carbon fiber leads. Some of the leads were shielded (standard copper coaxial shielding) and we tested both when this shielding was connected to the common ground reference and when it was not. While carbon fiber has the advantage of being radio-translucent and is, therefore, less likely to experience induced currents, it is also more expensive and not as readily available. The end-connections to electrodes were either regular or snap-on, a type of connector that can be snapped on a socket pasted on a subject's skin. Given the large number of possible lead/electrode/end-connection combinations, we restricted ourselves to a smaller set of electrode types. However, the length of the electrode lead was fixed to 30 feet, since a variation in the length of the wire would modify the resonance properties of the whole system.

In order to limit the effect of variable geometry, the placement of the leads was also fixed. Across all experiments, leads immediately descended to the floor, then directly to the wave-guide, and into the control room.

#### **6.3.4 Heat insulation**

Even though our work was designed to prevent any risk of burn on the subject, we implemented additional safety measures. Because the induced voltage is directly proportional to the surface between the conductive loop (Faraday's law of induction), we twisted together each pair of wires and stuffed them into standard window insulation foam. In addition to keeping the two wires close together and reducing the risk of accidental coiling, it prevented direct contact of the wires on the subject's skin.

#### **6.3.5 Filter design**

We used two types of filters, a simple capacitor filter and a third-order pi filter. These filters were placed in line with the electrode leads inside the MRI control room (see the box marked 'filters' in Figure 6-1). The simple filter type consisted of a 10pF capacitor between each wire of a lead pair (Figure 6-2). At high frequencies, the capacitor behaves as a simple wire and effectively short circuits the two leads. This results in a low-pass filter, rejecting differential mode noise signal while keeping the low-frequency GSR recording. This type of filter; however, proved to be insufficient for our noise constraints, as the signal of interest was not clearly visible. A large amount of noise was common between the leads with this filter.

The second type of filter was a standard third-order pi design diagrammed in Figure 6-3. The filter response with loadings of 30 k $\Omega$  on both ends is displayed on Figure 6-4. The main safety issue with this design is the need to have a connection to the ground. Connecting a subject to a non-isolated ground is regarded as dangerous because a voltage differential between two references can result in electric shock. We therefore used high voltage capacitors (rated 3kV) to prevent such risks. This practice was suggested by the international norm IEC 60601-1.

For the second type of filter, we used two types of ground connection, the cage surrounding the scanner room, or a ground common to the Psylab hardware. In the first case, the filter should reduce the noise on the skin-conductance measurements, but in the second case there is additional electrical isolation (discussed in more detail in results below). It is most important that equipment electrically connected to the measuring equipment be connected to the same ground to minimize any ground reference differences. We also minimized any line noise by using band-pass filtered power strips.

### **6.3.6 Head coils**

We used two types of head coils, as they could potentially modify the currents in the leads by modifying the characteristics of the magnetic field. The first type was the standard “bird cage” coil (CP Head, receive and transmit, Siemens Medical, Munich Germany). We also used a custom “8-channel” coil (receive only, MRI Devices, Orlando, FL). Because the scanner body coil is used as a transmitter while the 8-channel coil is used as a receiver only, this setup yields a better image quality but induces greater noise in attached electrodes.

### **6.3.7 Resonance testing**

The first safety test was performed outside the scanner utilizing a network analyzer (Agilent 8712ET 300kHz-1300MHz RF Network Analyzer, Agilent, Palo Alto, CA). Different parts of the installation were connected together except for the power supply, which was disconnected in order to test the passive properties of the circuit. By connecting the probe electrodes to the leads on the paste human model, we could sweep across a wide range of frequencies in order to detect resonances. Our rationale for this safety test was that the network analyzer injects frequencies in a fashion similar to the scanner magnetic field. If a circuit had presented a resonance at the scanner's Larmor frequency, it would be considered unsafe. Results are described below.

### **6.3.8 Measurement of induced voltages**

The second set of measurements was performed with all the equipment turned on. After placing the paste model into the scanner, we ran an EPI scan (T2\*-weighted PACE EPI TR=2000ms, TE=30ms, 64x64, 3.28125x3.28125 mm<sup>2</sup>, 32 3.0mm slices, no gap, field of view = 210) and measured the voltages between leads with a digital oscilloscope (TDS 5104 Digital Oscilloscope 1GHz 5GS/s, Tektronix, Richardson, TX). We took three measurements; the first was between the two leads of the SCR electrodes, the second one was between the two leads of the shocking electrodes, and the third one was between one lead of each type.

Since the sequence does not produce voltages between the leads continuously, a direct measurement cannot be taken. We increased the trigger level of the oscilloscope



until the trace was stable and then read both the peak and the root mean square (RMS) values directly. The peak values reflect the maximum instantaneous voltage received and the RMS values are a direct measure of the energy induced in the dummy.

It should be noted that we limited ourselves to EPI sequences during our measurements on the dummy, and that the leads should be disconnected when a human subject is scanned with another sequence or during shimming.

## **6.4 Results**

### **6.4.1 Resonances**

Figure 6-5 shows one example of a network analysis plot. The lack of a sharp dip around 123 MHz reveals that the circuit does not show specific resonance around the Larmor frequency, and that most of the energy injected into the circuit at that frequency is not absorbed (in this example the absorption is 2.4dB). We observed several other dips at other frequencies, but since they are far away from our operating range, we concluded that they presented no safety risks.

None of our various configurations presented any resonance around the Larmor frequency, and we therefore proceeded to the next step.

### **6.4.2 Recorded waveform**

Figure 6-6 shows a typical waveform recorded during an EPI sequence. One can see a group of two pulses that occur at repeated intervals. We matched this frequency with the number of slices acquired every second. The first pulse of the group is the fat-saturation pulse, while the second narrower pulse corresponds to a slice selection pulse.

By increasing the time resolution, we can look into the larger amplitude of the two, the slice selection pulse. The measured frequency matches ~123 MHz. This confirms that the signal we recorded is induced by the scanner and is the one to be investigated to test the safety of the installation.

### **6.4.3 Recorded voltages**

We then proceeded by repeatedly recording the voltages induced during the slice selection sequence. Three main parameters were identified: type of filter, type of head coil and type of lead. Among all combinations tested, no measurement was above 3000mV, which, with a skin conductance of about 30k $\Omega$ , would create a current of 0.1mA, generally considered below detectable limits.

Two types of head coils were used: standard “bird cage” and high quality “8 channel,” as shown in Table 1, Section 1. Results indicate that modification of the magnetic fields greatly changes the induced voltages on the leads. The values recorded when using the bird cage coil (top three rows) are significantly below ( $p < 0.001$  in all cases) the ones when using the 8-channel coil (bottom three rows). The bird cage is a receive/transmit coil that probably confines most of the variable magnetic field to a region close to the head. The 8-channel coil, being only a receiver, uses the magnet’s coils as transmitter and therefore yields a higher variable field near the hands. Even though the 8-channel coil yields higher voltages, the values are minimal and its use is still safe. Therefore, we chose to use it over the bird cage, as it provides superior fMRI recordings.

Section 2 of Table 6-1 shows the effect of the different leads. The carbon fiber leads seem to display the lowest induction and we believe that, unless one is concerned with their relatively low conductance (resistance of 200  $\Omega$  for 1 m) or their higher cost, they should be used. We can also note that the shielding lowers the inducted voltage if properly grounded.

We measured voltages (see Table 6-1, Section 3) for two types of filters. Even though the filters were designed to improve the quality of the recordings, they are a parameter when it comes to subjects' safety. The two ground connections for the type-2 filter do not modify the recorded values significantly. This may have been due to remaining ground reference differences. As the type-1 filter neither provides better quality signal nor lower induced voltages, we do not recommend its use unless one does not want a connection to the ground at any cost.

#### **6.4.4 GSR recording quality**

Figure 6-7 displays a typical GSR recording showing the onset of EPI scans. The first part of the figure shows a typical skin conductance recording while the second part depicts a recording during an EPI scan, the onset of the scanning being marked with a vertical line. The first recordings were of poor quality due to the presence of interference from other electronic equipment and bad lead connections. However, a careful set-up leads to much higher signal quality, and this configuration yielded an SCR signal with very little noise.

## **6.5 Discussion**

Many investigation techniques in neuroscience, such as EEG and ECG recording, skin conductance measurements, or the delivery of shocks, are useful for investigations in neuroscience. However, recording in conjunction with fMRI scanning presents safety risks and adds noise that requires signal filtering. In this chapter, we presented a method to evaluate the safety of a complete recording system. All values point toward induced currents that are well below safety requirements. In addition, the filter presented eliminates most of the noise induced by the scanner, although further digital filtering can be applied.

This procedure for safety testing can be easily reproduced for other systems. Even though it appears that this type of analysis is rarely done, the effect of the leads, filters, or head coil shown above prove that any system should be tested prior to use on human subjects. The measurements can be reproduced to provide early testing of any biological recording system.

## 6.6 Tables

Table 6-1

		Peak		RMS	
		Mean	STD	Mean	STD
Bird cage	SHK	76.1	7.9	19.8	5.6
	GSR	89.8	5.1	39.2	5.4
	XRS	206.4	12.6	86.9	2.7
8 channel coil	SHK	733	155.8	383.3	89.8
	GSR	588	82.9	283.2	41.1
	XRS	305	24.3	117.6	15.7

*filter 1 / carbon fiber leads*

		Peak		RMS	
		Mean	STD	Mean	STD
Copper leads	SHK	1264	23.9	466.6	27.3
	GSR	382.4	13.1	185.1	8
	XRS	2176	61.4	982	39.3
Carbon fiber extension	SHK	998	42	474.4	30.2
	GSR	485	41.5	240.7	31.3
	XRS	579.6	11.7	264.2	4.9
Shielded snap leads	SHK	2446	111.8	1523.8	62.7
	GSR	1174	26.8	588.5	26.4
	XRS	784	46.6	350.8	23.8
Snap leads	SHK	732	71.2	326	40.4
	GSR	1512	20.9	781.8	28.2
	XRS	307.4	26.7	241.5	7.3
Carbon fiber leads	SHK	733	155.8	383.3	89.9
	GSR	588	82.9	283.2	41.1
	XRS	305	24.3	117.6	15.7

*8 channel coil / filter 1*

		Peak		RMS	
		Mean	STD	Mean	STD
Filter 1	SHK	773	155.8	383.3	89.8
	GSR	558	82.9	283.2	41.1
	XRS	305	24.3	117.6	15.7
Filter 2 - room ground	SHK	336.6	23.2	164	32.5
	GSR	266.8	6.5	128.8	5.4
	XRS	224.8	19.4	103.8	10.3
Filter 2 - isolated ground	SHK	335.2	6.8	164.6	4.3
	GSR	316.4	13.6	149.2	7.7
	XRS	188	20.4	89.4	9.6

*8 channel coil / carbon fiber leads*

Table 6-1 Comparison of the effect of the head coil: We measured the peak and RMS voltages (in milivolts) for different configurations. The probe leads were connected between the two shock leads (SHK), the two skin conductance leads (GSR), or between one shock lead and one skin conductance lead (XRS). Measures were taken repeatedly and we reported the mean value (left column) and the standard deviation (right column). The first part of the table describes the effect of the head-coils, the second part the effect of the leads, and the third part the effect of the filters.

Figures

**Figure 6-1**

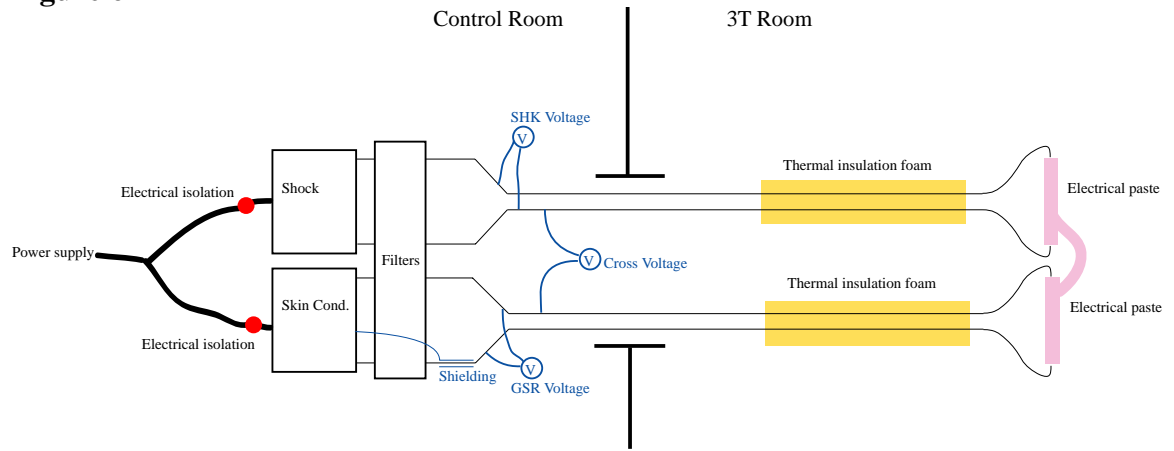
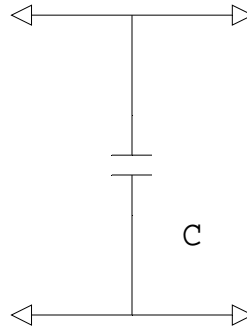
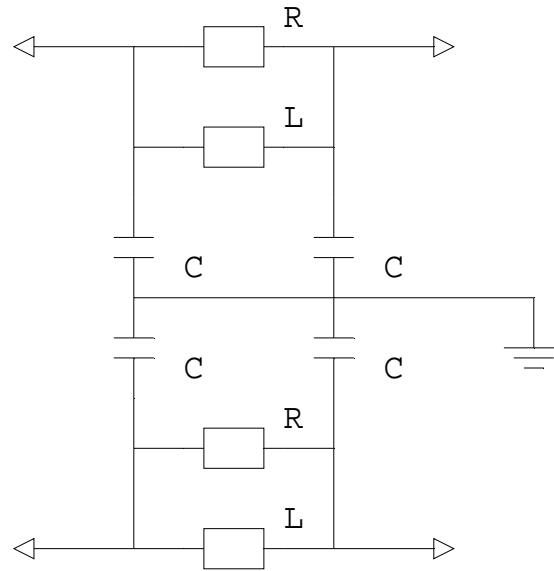


Diagram of the experimental setup

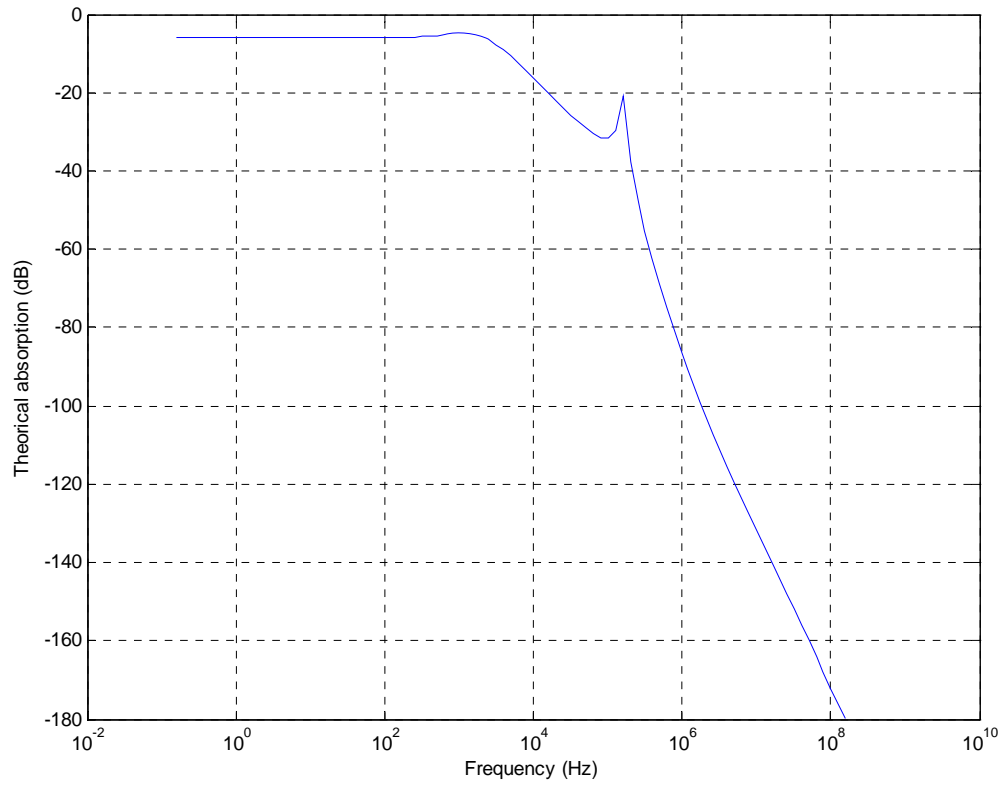
**Figure 6-2**

Filter 1: Simple filter connected between the two leads that are connected to the skin conductance device. An identical filter is also used between the leads of the shocking device ( $C=10\text{pF}$ ). Filter positions in the experimental setup are indicated in Figure 6-1 in the box marked “filters”. One filter pair would be located in the top half of the box and one in the lower half of the box. Filter orientation is such that the simulated subject would be on the right and the control system would be on the left.

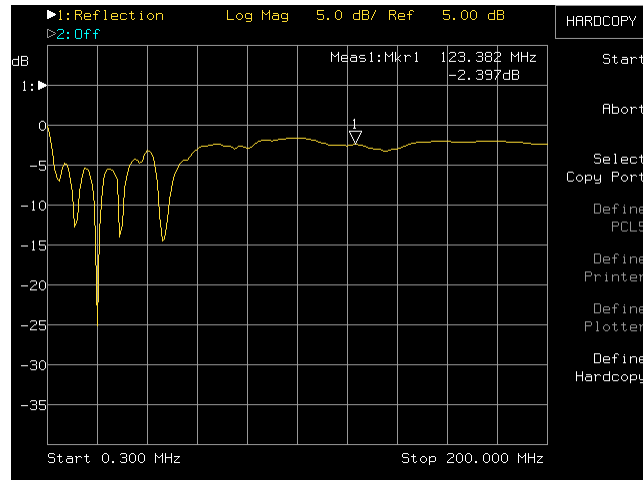


**Figure 6-3**

Filter 2: Pi-filter connected between the two leads that are connected to the skin conductance device. An identical filter is also used between the leads of the shocking device. The grounds of both filters are connected together and then connected to an isolated ground on the Psylab box ( $C = 1\text{nF}$ ,  $R=10\text{k}\Omega$ ,  $L=10\text{mH}$ ). Filter positions in the experimental setup are indicated in Figure 6-1 in the box marked “filters”. One filter pair would be located in the top half of the box and one in the lower half of the box. Filter orientation is such that the simulated subject would be on the right and the control system would be on the left.

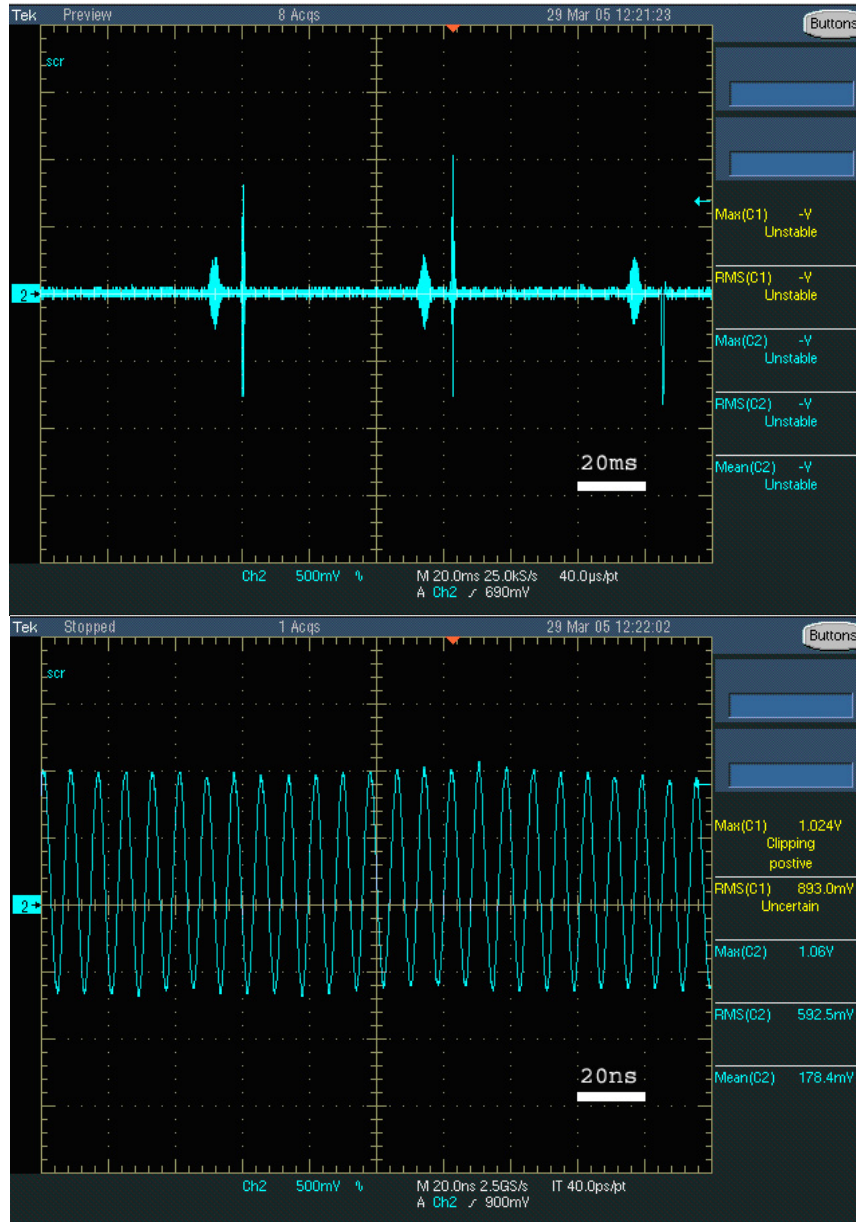
**Figure 6-4**

Theoretical response of the type-2 filter

**Figure 6-5**

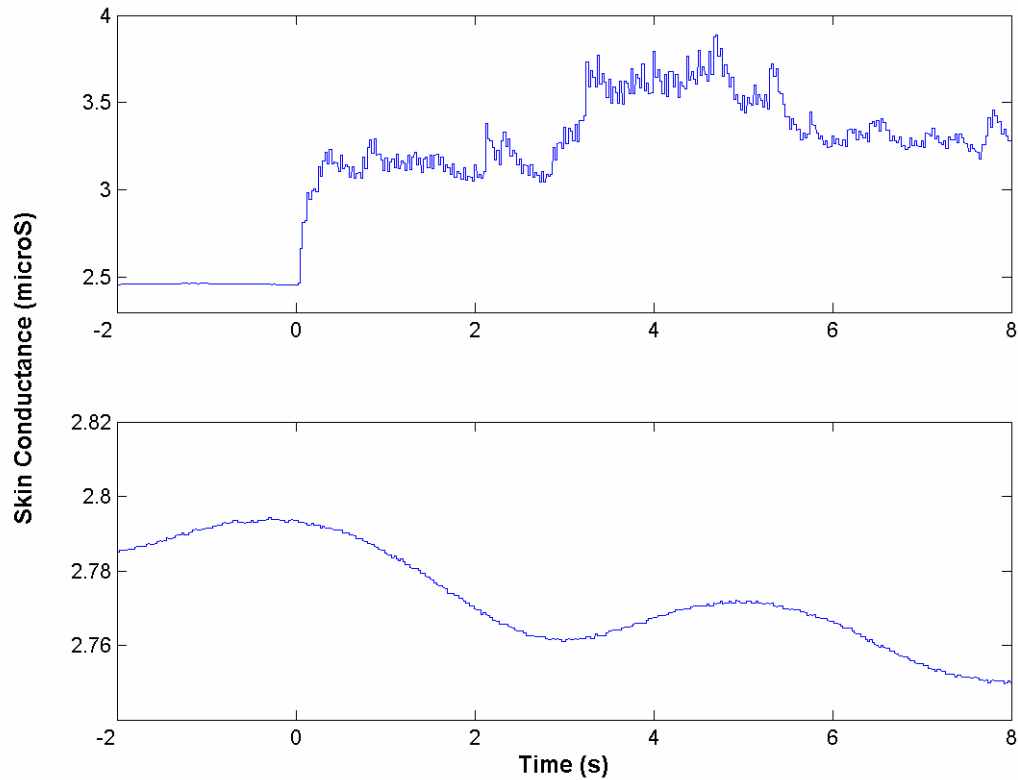
Typical resonance response, GSR with snap leads: The cursor is located at the Larmor frequency (horizontal axis ranging from 0.3 MHz to 200 MHz) and the reflected power is measured in dB (vertical axis ranging from 1 to -40 dB)

Figure 6-6



Typical induced voltages on the leads: The top snapshot displays the repetition of a slice acquisition. The bottom snapshot is a time-magnification that shows the oscillations of the magnetic fields during the slice selection pulse exhibited at the Larmor frequency.

Figure 6-7



Skin conductance recording during EPI scanning, using a full carbon fiber electrode configuration with (bottom) and without optimizations (top). Optimizations of the skin conductance trace shown in the lower half included the use of the low pass filter in Figure 6-3, connecting all components to a common ground reference, and attention to placement of components within the control room. The onset of EPI scanning occurs approximately at zero seconds.